Flyover Bridge Formation via a Reversible C–C Coupling in Reactions of Diruthenium Pyridine-2-carbaldimine Complexes with Alkynes[1,2]

Fred Muller, Gerard van Koten, Louis H. Polm, Kees Vrieze,* and Martin C. Zoutberg

Laboratorium voor Anorganische Chemie, Universiteit van Amsterdam, J. H. van't Hoff Instituut, Nieuwe Achtergracht 166, 1018 WV Amsterdam, The Netherlands

Dick Heijdenrijk, Edith Kragten, and Casper H. Stam

Laboratorium voor Kristallografie, Universiteit van Amsterdam, J. H. van't Hoff Instituut, Nieuwe Achtergracht 166, 1018 WV Amsterdam, The Netherlands

The reactions of $Ru_2(CO)_6$(*i*-Pr-Pyca) (**1a**) [*i*-Pr-Pyca = pyridine-2-carbaldimine] with ethyne, methyl propynoate (MP), and dimethyl acetylenedicarboxylate (DMADC) and the reaction of $Ru_2(CO)_6$(*t*-Bu-Pyca) (**1b**) with *p*-tolylacetylene (PTA) were studied. The reaction of **1a** with MP and DMADC leads to C–C coupling between the Pyca and the alkyne via a direct attack of one of the alkyne C atoms on the η^2-C=N coordinated imine moiety of **1**. In the resulting complex $Ru_2(CO)_6\{C_5H_4NCH(N$-*i*-Pr$)C(C(O)OMe)$=CR$\}$ [**2a**, R = C(O)OMe; **2b**, R = H], in which the Ru–Ru bond is absent, the second alkyne C atom is σ-bonded to the Ru center to which both N atoms are bonded and the reduced alkyne bond is η^2-C=C coordinated to the second Ru center. Complex **2a** thermally rearranges to $Ru_2(CO)_6$(*i*-Pr-Pyca)(μ_2-DMADC) (**3**), of which the crystal structure has been determined. Red crystals of **3** ($Ru_2C_{21}H_{18}N_2O_{10}\cdot0.5CH_2Cl_2$, Z = 4) are triclinic, space group $P\bar{1}$, and have cell constants a = 15.853 (3) Å, b = 17.221 (4) Å, c = 9.953 (2) Å, α = 91.40 (1)°, β = 95.56 (1)°, and γ = 86.03 (2)°. A total 7113 reflections (Mo Kα, μ = 12.50 cm^{-1}) were used in the refinement which converged to a final R value of 0.055. The structure shows a $Ru(CO)_4$ and a $Ru(CO)_2$(*i*-Pr-Pyca) fragment (all CO ligands are terminally bonded) which are bridged by a μ_2-parallel bonded DMADC molecule and linked by a formally single Ru–Ru bond of 2.899 (3) Å. Complex **3** reacts thermally with a second DMADC to give $Ru_2(CO)_4$(*i*-Pr-Pyca)$\{(C(C(O)OMe)$=C(C(O)OMe)$)_2C$=O)$\}$ (**4a**), of which the crystal structure has also been determined. Yellow crystals of **4a** ($Ru_2C_{26}H_{24}N_2O_{13}\cdot C_4H_8O\cdot CH_2Cl_2$, Z = 4) are monoclinic, space group $P2_1/n$, and have cell constants a = 20.610 (3) Å, b = 15.521 (2) Å, c = 11.552 (1) Å, and β = 92.80 (1)°. A total of 6529 reflections (Mo Kα, μ = 10.13 cm^{-1}) were used in the refinement which converged to a final R value of 0.064 (R_w = 0.103). The structure consists of a Ru(CO)(*i*-Pr-Pyca) and a $Ru(CO)_3$ fragment linked by a formally single Ru–Ru bond of 2.7630 (6) Å and bridged by a flyover ligand formed by the C–C coupling of two DMADC molecules to a CO group. The ligand is bonded to each Ru center via a Ru–C σ-bond and an η^2-C=C bonded olefinic fragment. The reaction of **1a** with MP at 98 °C gives $Ru_2[MeOC(O)C$=CHC(C(O)OMe)$=CH](CO)_4$(*i*-Pr-Pyca) (**7**), which is the first ruthenacyclopentadienyl α-diimine complex. The Pyca ligand is bonded to the Ru in the metallacycle while one of the CO ligands is bridging. The thermal reactions of **1a** with ethyne and **1b** with PTA yield complexes $Ru_2(CO)_4$(R-Pyca)$\{HC$=C(R′)C(=O)C(R′)$=CH\}$ (**4b**, R = *t*-Bu, R′ = *p*-Tol; **4c**, R = *i*-Pr, R′ = H) which are isostructural with **4a**. The crystal structure of **4b** has been established. Dark red crystals of **4b** ($Ru_2C_{33}H_{30}N_2O_5$, Z = 4) are monoclinic, space group Cc, and have cell constants a = 14.622 (4) Å, b = 22.381 (5) Å, c = 12.687 (12) Å, and β = 116.99 (4)°. A total 1405 reflections (Mo Kα, μ = 8.35 cm^{-1}) were used in the refinement which converged to a final R value of 0.054 (R_w = 0.116). Complexes **4a** and **4b** are the first Ru flyover complexes that have been crystallographically characterized. The product **4c** consists of a mixture of three isomeric complexes which differ with respect to the orientation of the Pyca ligand relative to the pentadienonediyl fragment.

Introduction

The chemistry of transition-metal complexes of α-diimines is dominated by the versatile coordination behavior of this type of organic ligands.[3] This versatility originates from the availability for coordination of two N lone pairs as well as the π-systems of the two C=N bonds. The most important coordination modes in dinuclear complexes are the σ,σ-N,N′ chelating 4e donating,[4] the σ-N,μ_2-N′,η^2-C=N′ bridging 6e donating,[5] and the σ,σ-N,N′-η^2,η^2-C=N,C=N′ bridging 8e donating[6] bonding modes. The most frequently studied α-diimine ligands are R-DAB (1,4-diaza-1,3-butadiene; RN=CHCH=NR), R-Pyca (pyridine-2-carbaldimine; C_5H_4N-2-CH=NR), and 2,2′-bipyridine. These three types of α-diimine ligands differ in the decreasing π-acceptor capacity as well as with respect to the number of possible coordination modes and the decreasing possibility to donate electrons, since the N=C fragments

that are part of an aromatic pyridyl system cannot be η^2-C=N coordinated due to the resulting loss of resonance stabilization. This loss of resonance stabilization is also

(1) Reactions of Dinuclear Metal Carbonyl α-Diimine Complexes with Alkynes. 10. Part 9: see ref 2.

(2) Muller, F.; Dijkhuis, D. I. P.; van Koten, G.; Vrieze, K.; Heijdenrijk, D.; Rotteveel, M. A.; Stam, C. H.; Zoutberg, M. C. *Organometallics*, in press.

(3) (a) van Koten, G.; Vrieze, K. *Adv. Organomet. Chem.* **1982**, *21*, 151. (b) Vrieze, K. *J. Organomet. Chem.* **1986**, *300*, 307. (c) van Koten, G.; Vrieze, K. *Recl. Trav. Chim. Pays-Bas* **1981**, *100*, 129. (d) van Koten, G.; Vrieze, K. *Inorg. Chim. Acta* **1985**, *100*, 79. (e) Kokkes, M. W.; Stufkens, D. J.; Oskam, A. *Inorg. Chem.* **1985**, *24*, 4411.

(4) Muller, F.; Vrieze, K. *Coordination Chemistry and Catalysis*; Ziolkowski, J. J., ed.; World Scientific Publishing Co.: Singapore, 1988.

(5) (a) Frühauf, H.-W.; Landers, A.; Goddard, R.; Krüger, K. *Angew. Chem.* **1978**, *90*(1), 56. (b) Zoet, R.; van Koten, G.; Muller, F.; Vrieze, K.; van Wijnkoop, M.; Goubitz, K.; van Halen, C. J. G.; Stam, C. H. *Inorg. Chim. Acta* **1988**, *149*(2), 193.

(6) (a) Keijsper, J.; Polm, L. H.; van Koten, G.; Vrieze, K., Abbel, G.; Stam, C. H. *Inorg. Chem.* **1984**, *23*, 2142. (b) Staal, L. H.; van Koten, G.; Vrieze, K.; Ploeger, F.; Stam, C. H. *Inorg. Chem.* **1981**, *20*, 1830. (c) Part 1 of this series: Muller, F.; van Koten, G.; Vrieze, K.; Heijdenrijk, D. *Inorg. Chim. Acta* **1989**, *158*, 81.

* To whom correspondence should be addressed.

Table I. IR and Mass Spectroscopy Data and Elemental Analyses of $Ru_2(CO)_6[APP(i\text{-Pr,R,R'})]$ (2a, R = R' = C(O)OMe; 2b, R = C(O)OMe, R' = H), $Ru_2(CO)_6(i\text{-Pr-Pyca})(\mu_2\text{-DMADC})$ (3), $Ru_2(CO)_4(R\text{-Pyca})[R'C\!=\!CR''C(\!=\!O)CR''\!=\!CR']$ (4a, R = i-Pr, R' = R'' = C(O)OMe; 4b, R = t-Bu, R' = H, R'' = p-Tol; 4c, R = i-Pr, R' = R'' = H), and $Ru_2[MeOC(O)C\!=\!CHC(C(O)OMe\!=\!CH](CO)_4(i\text{-Pr-Pyca})$ (7)

compd	IR ν_s(C=O),[a] cm^{-1}	FI/FD mass (calcd)[b]	C obsd	C calcd	H obsd	H calcd	N obsd	N calcd
2a	2096 (s), 2059 (vs), 2021 (s), 1988 (s), 1973 (s), 1691 (s)	661 (660.51)	38.52	(38.19)	3.36	(2.75)	4.12	(4.24)
2b	2087 (m), 2049 (s), 2022 (s), 1979 (s, b), 1726 (w)	603 (602.47)	37.66	(37.88)	2.73	(2.68)	4.78	(4.65)
3	2079 (s), 1993 (vs, b), 1937 (s), 1678 (s)	... (660.51)	38.52	(38.19)	2.78	(2.75)	4.12	(4.24)
4a	2074 (s), 2041 (s), 2022 (s), 1967 (s, b), 1695 (s, b)	775 (774.61)	40.11	(39.96)	3.55	(3.76)	3.25	(3.01)[c]
4b	2054 (s), 1989 (s, b), 1926 (m), 1640 (m)	735 (736.72)	53.84	(53.80)	4.15	(4.10)	3.50	(3.80)
4c	2042 (s), 1986 (s), 1961 (s), 1937 (s), 1656 (m)	543 (542.46)	40.32	(39.85)	3.19	(2.97)	5.06	(5.16)[d]
7	2004 (s), 1976 (s), 1930 (s), 1814 (s), 1678 (s)	631 (630.52)	40.25	(40.00)	3.26	(3.20)	4.45	(4.44)

[a] Measured in CH_2Cl_2 solution. Abbreviations: vs, very strong; s, strong; m, medium; w, weak; vw, very weak; b, broad. [b] Based on ^{101}Ru. [c] Calculated for $Ru_2(CO)_4(i\text{-Pr-Pyca})(C_2(C(O)OMe)_2C(\!=\!O)C_2(C(O)OMe)_2)\cdot THF\cdot CH_2Cl_2$. [d] Analysis of a mixture of 4c,c',c''.

the reason that 2,2'-bpy does not give the C–C or C–N coupling reactions, which are observed for the CH=NR group of R-Pyca and both imine fragments of R-DAB.

The type of α-diimine complex of which the reactivity has been studied most extensively is $Ru_2(CO)_6(R\text{-DAB})$, in which the R-DAB ligand is bonded as a $\sigma\text{-N},\mu_2\text{-N'},\eta^2\text{-}C\!=\!N'$ bridging 6e donor. Reactions of this complex with unsaturated organic substrates have resulted in a number of C–C and C–N coupling reactions involving the $\eta^2\text{-}C\!=\!N$ coordinated imine moiety. This has been ascribed to the activation of the latter fragment by metal-to-ligand π-back-bonding that is a key factor for these C–C and C–N couplings to take place.[3] In the case of alkynes these coupling reactions appeared to result in a number of interesting further reactions involving sequential C–C coupling reactions and reversible metal–metal bond fission processes.[2,7] In order to obtain a better insight in these reactions the reactivity was studied of the isostructural complexes $M_2(CO)_6(L)$ [M_2 = Fe$_2$, FeRu, Ru$_2$; L = R-DAB, R-Pyca] toward a series of different alkynes.[8] In the first six parts of this series we reported reactions of the diiron complexes,[9] while parts 7 and 8 were devoted to the reactivity of the heterodinuclear $FeRu(CO)_6(i\text{-Pr-DAB})$ toward alkynes.[10] In a recent paper (part 9)[2] a detailed study of the reactions of $Ru_2(CO)_6(R\text{-DAB})$ with a number of alkynes was presented. This paper reports on the reactivity of the homodinuclear complexes $Ru_2(CO)_6(R\text{-Pyca})$ (1a, R = i-Pr; 1b, R = t-Bu)[11] toward ethyne, methyl propynoate (MP), dimethyl acetylenedicarboxylate (DMADC), and p-tolylacetylene (PTA). We were interested to compare these results with those of the reactions of the comparable R-DAB complexes, since the more rigid nature of the R-Pyca ligand in combination with a similar activation of the $\eta^2\text{-}C\!=\!N$ coordinated imine moiety may

lead to the stabilization of intermediates which cannot be isolated in the case of R-DAB. Furthermore a different reactivity of 1 when compared to $Ru_2(CO)_6(R\text{-DAB})$ is expected in reactions with ethyne. The latter complex reacts with ethyne via the initial decarbonylation to $Ru_2(CO)_5(R\text{-DAB(8e)})$, which actually reacts with ethyne to $Ru_2(CO)_4(i\text{-Pr-DAB(8e)})(\mu_2\text{-HC}\!=\!CH)$. Since the 8e coordination mode is not possible for R-Pyca (see above), the reaction of 1 with ethyne must proceed via another reaction path.

Experimental Section

Materials and Apparatus. ^{1}H and ^{13}C NMR spectra were obtained on Varian XL100, Bruker AC100, and Bruker WM250 spectrometers. IR spectra were measured with a Perkin-Elmer 283 spectrometer. The field desorption (FD) mass spectra were measured on a Varian MAT711 double-focusing mass spectrometer, fitted with a 10-μm tungsten FD emitter, containing microneedles with an average length of 30 μm, using emitter currents of 0–10 mA. The field ionization (FI) mass spectra were obtained with a Varian MAT711 double-focusing mass spectrometer with a combined EI/FI/FD source. The samples were dissolved in dichloromethane and introduced via the direct insertion probe into the ion source, of which the temperature was generally 60–160 °C. Elemental analyses were carried out by the section Elemental Analysis of the Institute for Applied Chemistry, TNO, Zeist, The Netherlands.

All preparations were carried out in an atmosphere of purified nitrogen, using carefully dried solvents. All column chromatography was performed by using silica gel (60 mesh, dried and activated before use) as the stationary phase. $Ru_2(CO)_6(R\text{-Pyca})$ (1a, R = i-Pr; 1b, R = t-Bu) was prepared according to known procedures.[11] Methyl propynoate (MP) and dimethyl acetylenedicarboxylate (DMADC) were distilled prior to use. Ethyne was used as commercially obtained. p-Tolylacetylene (PTA) was prepared according to literature methods.[12] The products were identified by IR and mass spectroscopy (Table I), and by ^{1}H NMR (Table II), and ^{13}C NMR (Table III).

Synthesis of $Ru_2(CO)_6[APP(i\text{-Pr,C(O)Me,R})]$[13] (2a, R = C(O)OMe; 2b, R = H). A solution of $Ru_2(CO)_6(i\text{-Pr-Pyca})$ (1a) (1 mmol, 518 mg, prepared in situ) and $RC\!\equiv\!CC(O)OMe$ (1 mmol, 84 mg (R = H), 142 mg (R = C(O)OMe)) in 50 mL of heptane was stirred at 20 °C for 48 h. The formed orange precipitate was filtered off, washed with three portions of 20 mL of hexane, and dried in vacuo (yield 40–60%).

Synthesis of $Ru_2(CO)_6(i\text{-Pr-Pyca})(\mu_2\text{-DMADC})$ (3). $Ru_2(CO)_6[APP(i\text{-Pr,C(O)Me,C(O)OMe})]$ (2a) (1 mmol, 660 mg) was refluxed for 1 h in 30 mL of dichloromethane during which

(7) Staal, L. H.; van Koten, G.; Vrieze, K.; van Santen, B.; Stam, C. H. *Inorg. Chem.* **1981**, *20*, 3598.

(8) Elsevier, C. J.; Muller, F.; Vrieze, K.; Zoet, R. *New. J. Chem.* **1988**, *12*, 571.

(9) (a) Part 2 of this series: Muller, F.; van Koten, G.; Vrieze, K.; Heijdenrijk, D. *Organometallics* **1989**, *8*, 33. (b) Part 3 of this series: Muller, F.; van Koten, G.; Vrieze, K.; Heijdenrijk, D.; Krijnen, L. B.; Stam, C. H. *Organometallics* **1989**, *8*, 41. (c) Part 4 of this series: Muller, F.; Han, I. M.; van Koten, G.; Vrieze, K.; Heijdenrijk, D.; de Jong, R. L.; Zoutberg, M. C. *Inorg. Chim. Acta* **1989**, *158*, 69. (d) Part 5 of this series: Muller, F.; Han, I. M.; van Koten, G.; Vrieze, K.; Heijdenrijk, D.; van Mechelen, J.; Stam, C. H. *Inorg. Chim. Acta* **1989**, *158*, 99. (e) Part 6 of this series: Muller, F.; van Koten, G.; Vrieze, K.; Heijdenrijk, D.; Duineveld, C. A. A.; Mak, A. N. S.; Stam, C. H. *Organometallics*, first of three papers in this issue.

(10) (a) Part 7 of this series: Muller, F.; van Koten, G.; Kraakman, M. J. A.; Vrieze, K.; Zoet, R.; Duineveld, C. A. A.; Heijdenrijk, D.; Stam, C. H.; Zoutberg, M. C. *Organometallics*, in press. (b) Part 8 of this series: Muller, F.; van Koten, G.; Kraakman, M. J. A.; Vrieze, K.; Heijdenrijk, D.; Zoutberg, M. C. *Organometallics*, second of three papers in this issue.

(11) Polm, L. H.; van Koten, G.; Elsevier, C. J.; Vrieze, K.; van Santen, B. F. K.; Stam, C. H. *J. Organomet. Chem.* **1986**, *304*, 353.

(12) Jacobs, T. L. *Organic Reactions*; Adams, R., ed.; John Wiley and Sons Inc.: London, 1949; Vol. 3 p 1.

(13) APP(R,R',R'') is the abbreviation for the organic ligand resulting from the C—C bond formation between an R-Pyca ligand and an alkyne R'C≡CR''. The backbone of the ligand is $C_5H_4N\text{-CH(NR)CR'}\!=\!CR''$, which is 2-amino-2-pyridinopropene.

Table II. ¹H NMR Data of Ru₂(CO)₆[APP(i-Pr,R,R')] (2a, R = R' = C(O)OMe; 2b, R = C(O)OMe, R' = H), Ru₂(CO)₆(i-Pr-Pyca)(μ₂-DMADC) (3), Ru₂(CO)₄(R-Pyca)[R'C═CR''C(═O)CR''═CR'] (4a, R = i-Pr, R' = R'' = C(O)OMe; 4b, R = t-Bu, R' = H, R'' = p-Tol; 4c, R = i-Pr, R' = R'' = H), and Ru₂[MeOC(O)C═CHC(C(O)OMe═CH](CO)₄(i-Pr-Pyca) (7)ᵃ

2aᵇ	1.32, 1.36 (d, d, 6 Hz, i-Pr Me); 2.28 (sept, 6 Hz, i-Pr CH); 3.47, 3.55 (s, s, OMe); 4.93 (s, N–CH); 6.70 (m), 7.51 (m), 8.32 (d, 5 Hz, pyridine)
2bᶜ	1.32, 1.34 (d, d, 6 Hz, i-Pr Me); 2.28 (sept, 6 Hz, i-Pr CH); 3.59 (s, OMe); 4.98 (s, N–CH); 6.78 (m), 7.45 (m), 8.04 (d, 6 Hz; pyridine); 9.09 (s, ═CH)
3ᶜ	1.53, 1.58 (d, d, 6 Hz, i-Pr Me); 3.68, 3.79 (s, s, OMe); 4.47 (sept, 6 Hz, i-Pr CH); 7.53 (m), 7.87 (m), 9.30 (d, 5 Hz, pyridine); 8.48 (s, N═CH)
4aᶜ	1.43 (d, 6 Hz, i-Pr Me); 3.10, 3.59, 3.68, 3.84 (4 × s, OMe); 4.75 (sept, 6 Hz, i-Pr CH); 7.46 (m), 7.77 (m), 9.56 (d, 6 Hz, pyridine); 8.43 (s, N═CH)
4bᵈ	1.65 (s, t-Bu); 2.06, 2.27 (s, s, p-Tol Me); 6.33, 6.48 (dd, 8 Hz, p-Tol); 7.02, 7.28 (dd, 8 Hz, p-Tol); 7.04, 7.27, 7.61, 8.72 (3 × m, d, 6 Hz, pyridine); 8.07 (s, N═CH); 8.85, 9.47 (s, s, ═CH)
4cᶜ	1.61 (d, 6 Hz, i-Pr Me); 4.85 (sept, 6 Hz, i-Pr CH); 4.24, 4.47 (dd, dd, 6 Hz, 2 Hz, HCC(═O)CH); 7.32, 7.99 (d, d, 6 Hz, ═CH); 7–8 (m), 8.50 (d, 5 Hz, pyridine); 8.59 (N═CH)
4c'ᶜ	1.29, 1.48 (d, d, 6 Hz, i-Pr Me); 4.15 (sept, 6 Hz, i-Pr CH); 3.36, 4.57 (dd, dd, 6 Hz, 2 Hz, HCC(═O)CH); 8.50, 8.68 (d, d, 6 Hz, ═CH); 7–8 (m), 8.93 (d, 5 Hz, pyridine); 8.59 (N═CH)
4c''ᶜ	1.43,1.61 (d, d, 6 Hz, i-Pr Me); 4.33 (sept, 6 Hz, i-Pr CH); 7–8 (m), 9.25 (d, 5 Hz, pyridine); 8.59 (N═CH)ᵉ
7ᶠ	1.49, 1.61 (d, d, 6 Hz, i-Pr Me); 3.39, 3.70 (s, s, OMe); 4.79 (sept, 6 Hz, i-Pr CH); 7.10, 7.40 (d, d, 2.8 Hz, ═CH); 7–8 (m), 8.75 (d, 5 Hz, pyridine); 8.39 (s, N═CH)

ᵃ ¹H NMR values in ppm relative to Me₄Si, measured in CDCl₃ solution, spectrometer frequency = 100 MHz. ᵇ T = 300 K. ᶜ T = 293 K. ᵈ T = 298 K, spectrometer frequency = 250 MHz. ᵉ Ethyne proton resonances not resolved. ᶠ T = 273 K.

Table III. ¹³C NMR Data of Ru₂(CO)₆[APP(i-Pr,R,R')] (2a, R = R' = C(O)OMe; 2b, R = C(O)OMe, R' = H), Ru₂(CO)₆(i-Pr-Pyca)(μ₂-DMADC) (3), Ru₂(CO)₄(R-Pyca)[R'C═CR''C(═O)CR''═CR'] (4a, R = i-Pr, R' = R'' = C(O)OMe; 4b, R = t-Bu, R' = H, R'' = p-Tol; 4c, R = i-Pr, R' = R'' = H), and Ru₂[MeOC(O)C═CHC(C(O)OMe═CH](CO)₄(i-Pr-Pyca) (7)ᵃ

2a	26.4, 28.3 (i-Pr Me); 50.8, 51.3 (OMe); 56.3 (═CR); 67.4 (i-Pr CH); 74.5 (N–CH); 119.3, 121.6, 137.4, 149.0, 156.7 (pyridine C⁵, C⁴, C³, C⁶, C²); 169.5, 171.6 (OC═O); 177.1 (═CRRu); 186.9, 192.1, 192.6, 194.6, 196.2, 199.1 (CO's) [T = 263 K, spectrometer frequency = 63 MHz]
2b	26.8, 28.5 (i-Pr Me); 52.3 (OMe); 66.3 (═CR); 67.5 (i-Pr CH); 75.3 (N–CH); 119.2, 121.6, 137.1, 149.0, 162.6 (pyridine C⁵, C⁴, C³, C⁶, C²); 170.2 (OC═O); 183.0 (═CH); 187.6, 193.1, 193.4, 195.6, 197.6, 200.7 (CO's) [T = 253 K]
3	22.9, 25.8 (i-Pr Me); 51.5, 51.8 (OMe); 64.6 (i-Pr CH); 126.5, 128.4, 136.9, 153.7, 156.2 (pyridine C⁵, C⁴, C³, C⁶, C²); 153.3 (2×, OC═O); 156.9 (N═CH); 168.7, 176.7 (RC═CR); 192.2, 205.0 (CO's) [T = 295 K]
4a	22.5, 25.1 (i-Pr Me); 50.4, 51.7, 51.8, 52.5 (OMe); 66.5 (i-Pr CH); 126.2, 137.9, 141.4, 149.6, 153.8 (pyridine C⁵, C⁴, C³, C⁶, C²); 139.4, 143.4 (C═CC(O)C═C); 160.3 (N═CH); 166.0, 168.2, 175.6, 176.2 (OC═O); 193.4, 195.7 (C═CC(O)C═C); 205.9 (C═CC(O)C═C); 206.3, 209.5, 212.8, 224.3 (CO's) [T = 303 K]
4b	21.0, 21.3 (p-Tol Me); 31.5, 64.7 (t-Bu); 88.9, 98.0 (C═CC(O)C═C); 125.4, 127.1, 127.8, 128.7 (p-Tol CH); 125.6, 126.1, 136.4, 152.9, 154.4 (pyridine C⁵, C⁴, C³, C⁶, C²); 133.0, 133.2 (p-Tol CMe); 135.6, 137.8 (p-Tol C); 157.8, 159.6 (C═CC(O)C═C); 158.5 (N═CH); 196.5 (C═CC(O)C═C); 201.7 (CO's) [T = 303 K]
4c	22.8, 25.6 (i-Pr Me); 57.7 (i-Pr CH); 74.5, 75.4 (C═CC(O)C═C); 125.6, 126.7, 136.2, 149.6, 151.8 (pyridine C⁵, C⁴, C³, C⁶, C²); 154.0, 154.4 (C═CC(O)C═C); 158.6 (N═CH); 199.1 (C═CC(O)C═C); 210.2 (CO's) [T = 293 K]
7	21.7, 25.4 (i-Pr Me); 51.8, 52.2 (OMe); 58.9 (i-Pr CH); 119.1, 119.9, 127.1, 137.8, 155.2 (pyridine C⁵, C⁴, C³, C⁶, C²); 127.5 (RC═CHCR═CH); 136.9 (RC═CHCR═CH); 156.2 (RC═CHCR═CH); 159.5 (RC═CHCR═CH); 175.5, 177.2 (OC═O); 192.8 (CO's) [T = 273 K]

ᵃ Values in ppm relative to Me₄Si, measured in CDCl₃ solution, spectrometer frequency = 25 MHz.

the color of the solution slowly changed from dark orange to red. The conversion was completed when in the IR spectrum of the reaction mixture (ν₈(C═O) region) the bands due to 2a had disappeared. The crude reaction product was purified by column chromatography. Elution with CH₂Cl₂/THF (1:1) produced 3 as a red solution in 80% yield. Crystallization from a CH₂Cl₂ solution at −80 °C produced dark red crystals suitable for X-ray crystallography. The crystals were collected by decanting the mother liquor, washed with 30 mL of hexane, and dried in vacuo. A virtually quantitative conversion of 2a to 3 was achieved by performing the reaction at 20 °C, although in this case the conversion is completed only after several days.

Synthesis of Ru₂(CO)₄(i-Pr-Pyca){(C(C(O)OMe)═C(C(O)OMe))₂C(═O)} (4a). A solution of 3 (0.5 mmol, 330 mg) and DMADC (0.5 mmol, 71 mg) in 30 mL of CH₂Cl₂ was refluxed for 30 min, during which the color of the solution gradually changed from red to orange-yellow. The crude reaction product was purified by column chromatography. Elution with THF produced 4a as a yellow solution in 80% yield. Crystals suitable for X-ray crystallography were obtained by crystallization from a CH₂Cl₂/THF (1:1) solution at −30 °C. The crystals were collected by decanting the mother liquor, washed with 30 mL of hexane, and dried in vacuo.

Synthesis of Ru₂(CO)₄(t-Bu-Pyca){(C(H)═C(p-Tol))₂C(═O)} (4b). A solution of 1b (1.5 mmol, 807 mg, prepared in situ) and PTA (5 mmol, 580 mg) in 50 mL of heptane was refluxed for 3 h, during which the color of the reaction mixture changed from orange-yellow to brown-red. The crude reaction mixture was separated by column chromatography. Elution with hexane/diethyl ether (1:4) produced a brown solution of a small amount of the as yet structurally unidentified complex Ru₂(CO)₅(t-Bu-Pyca)(PTA). Further elution with the same eluent produced 4b as a brown-red solution in 25–30% yield. Finally, elution with diethyl ether yielded Ru₂(CO)₅[APE(t-Bu)][11] in 20% yield. Crystals of 4b suitable for X-ray crystallography were obtained by crystallization from diethyl ether at −80 °C. The crystals were

collected by decanting the mother liquor, washed with 30 mL of hexane, and dried in vacuo.

Reaction of Ru₂(CO)₆(i-Pr-Pyca) (1a) with Ethyne. Through a refluxing solution of 1a (1.5 mmol, 777 mg, prepared in situ) in 50 mL of heptane was bubbled a gentle stream of ethyne. Immediately a red precipitate was formed. After about half an hour when in the IR spectrum (ν₈(C═O) region) of the reaction mixture the bands due to 1a had disappeared, the reaction was stopped. The mixture was cooled to 20 °C, and the precipitate was collected on a sintered glass filter. The crude product was purified by column chromatography. Elution with THF produced a red solution which contained, as was shown by ¹H NMR, a mixture of 4c,c',c'' (in a 2:1:1 ratio) with a total yield of 70–80%. Recrystallization from heptane/THF (1:1) at −80 °C produced a red microcrystalline solid that was collected by decanting the mother liquor, washed with 30 mL of hexane, and dried in vacuo.

Synthesis of Ru₂[C(C(O)OMe)═CHC(C(O)OMe)═CH](CO)₄(i-Pr-Pyca) (7). A solution of 1a (1 mmol, 518 mg, prepared in situ) and MP (3 mmol, 252 mg) in 50 mL of heptane was refluxed. The orange-yellow color of the solution gradually changed to brown-red, and a dark precipitate was formed. When after about 2 h in the IR spectrum (ν₈(C═O) region) of the reaction mixture the bands due to 1a had disappeared, the reaction was stopped. The solvent was removed in vacuo and the crude reaction mixture was separated by column chromatography. Elution with diethyl ether produced a small amount (yield < 10%) of the orange complex 2b. Further elution with CH₂Cl₂/THF (1:1) produced a red-brown solution that contained complex 7 in 40–50% yield. Crystallization from hexane/CH₂Cl₂ (1:1) at −80 °C produced a red-brown solid that was washed with 20 mL of hexane and dried in vacuo.

Table IV. Crystallographic Data of Ru₂(CO)₆(*i*-Pr-Pyca)(μ₂-DMADC) (3), R₂(CO)₄(*i*-Pr-Pyca){C₂(C(O)OMe)₂ C(=O)C₂(C(O)OMe)₂} (4a), and Ru₂(CO)₄(*t*-Bu-Pyca){HC=C(*p*-Tol)C(=O)C(*p*-Tol)=CH} (4b)

	3	4a	4b
formula (mol wt)	Ru₂C₂₁H₁₈N₂O₁₀ (660.51)	Ru₂C₂₆H₂₄N₂O₁₃ (774.61)	Ru₂C₃₃H₃₀N₂O₅ (736.72)
cryst system	triclinic	monoclinic	monoclinic
space group	P1̄	P2₁/n	Cc
a, Å	15.853 (3)	20.610 (3)	14.622 (4)
b, Å	17.221 (4)	15.521 (2)	22.381 (5)
c, Å	9.953 (2)	11.552 (1)	12.687 (12)
α, deg	91.40 (1)	90	90
β, deg	95.56 (1)	92.80 (1)	116.99 (4)
γ, deg	86.03 (2)	90	90
V, Å³	2697.7	3691.0	3699.9
d_{calcd}, g·cm⁻³; Z	1.73; 4	1.68; 4	1.32; 4
μ, cm⁻¹	12.50	10.13	8.35
color; size, mm³	red; 0.3 × 0.23 × 0.15	yellow; 0.25 × 0.33 × 0.35	red; 0.2 × 0.13 × 0.1
radiatn	Mo Kα, λ = 0.710 69 Å	Mo Kα, λ = 0.710 69 Å	Mo Kα, λ = 0.710 69 Å
2θ range, deg	2.2–40	2.2–60	2.2–56
no. of reflctns	11676	11063	9093
no. of reflctns with $I < 2.5\sigma(I)$	4563	4534	7688
no. of reflctns in refinement	7113	6529	1405
h min, max	−20, 20	−28, 28	−15, 15
k min, max	−21, 21	0, 28	0, 27
l min, max	0, 12	0, 16	0, 15
abs corr	DIFABS[15]	DIFABS[15]	DIFABS[15]
extinctn corr	isotropic	isotropic	none
weighting scheme	unit weights	$w = 1/(5.90 + F_o + 0.0187F_0^2)$	$w = 1/(6.28 + F_o + 0.064F_0^2)$
anomalous scattering	Ru, Cl	Ru	Ru
final R, R_w	0.055, ...	0.064, 0.103	0.054, 0.116

Crystal Structure Determinations of Ru₂(CO)₆(*i*-Pr-Pyca)(μ₂-DMADC) (3), Ru₂(CO)₄(*i*-Pr-Pyca){MeOC(O)C=C(C(O)OMe)C(=O)C(C(O)OMe)=CC(O)OMe} (4a), and Ru₂(CO)₄(*t*-Bu-Pyca){HC=C(*p*-Tol)C(=O)C(*p*-Tol)=CH} (4b). The crystallographic data for the complexes 3, 4a, and 4b are listed in Table IV. The reflections were measured on a Nonius CAD4 diffractometer (25 °C, θ–2θ scan) using grahite-mono-chromated Mo Kα radiation. Those with an intensity below the 2.5σ(*I*) level were treated as unobserved. The structures were solved by means of the heavy-atom method. The Ru atoms of 3 were located by using the symbolic addition program set SIM-PEL.[14] The Ru atoms of 4a and 4b were located by means of an E²-Patterson synthesis. The C, N, and O atomic positions were derived from ΔF–Fourier syntheses. The positions of the H atoms of 3 and 4a were calculated and not refined; the H atoms of 4b were excluded. The refinement of the non-hydrogen atoms proceeded by using anistropic block-diagonal least-squares calculations. An empirical absorption correction (DIFABS)[15] was applied. The calculations were performed with XRAY76,[16] the atomic scattering factors were taken from Cromer and Mann (1968),[17] and the dispersion correction factors from ref 18.

The unit cell of 3 appeared to contain two molecules of CH₂Cl₂, of which the C and Cl atomic parameters were refined aniso-tropically. The H atoms were calculated and not refined. The asymmetric unit of 4a contains one molecule of CH₂Cl₂ and one molecule THF. The C, Cl, and O atoms were refined isotropically; the H atoms were calculated and not refined.

Results and Discussion

The reactions discussed in this paper are schematically shown in Scheme I. The reactions of Ru₂(CO)₆(*i*-Pr-Pyca) (1a), in which the Pyca ligand is coordinated as a σ-

N,μ₂-N′,η²-C=N′ bridging 6e donor, with dimethyl acety-lenedicarboxylate (DMADC) or methyl propynoate (MP) at 20 °C give in high yield the complexes Ru₂(CO)₆[APP-[*i*-Pr,C(O)OMe,R)][13] (2a, R = C(O)OMe; 2b, R = H). The APP ligand is formed via the C—C coupling of the C atom of the η²-C=N bonded imine moiety in 1a with one of the alkyne C atoms, which in the case of MP involves the unsubstituted alkyne C atom. This type of ligand is structually comparable and isoelectronic with the AIB-(R,R′,R″)[19] ligands formed in many reactions of Ru₂-(CO)₆(R-DAB) with alkynes via the C–C coupling of the alkyne with the R-DAB ligand.[19] The resulting complexes Ru₂(CO)₆[AIB(R,R′,R″)][2] are isostructural to 2. The crystal structure of Ru₂(CO)₆[AIB(*t*-Bu,CF₃,CF₃)] showed that one of the alkyne C atoms is C–C coupled to the coordinated imine C atom and that the other alkyne C atom is σ-bonded to the Ru center to which both N atoms are bonded. The reduced alkyne bond is η²-C=C coor-dinated to the other Ru center. Since the AIB ligand donates eight electrons to the Ru₂(CO)₆ unit, instead of the six electrons donated by the R-DAB ligand, there is no Ru–Ru bond anymore, which is also clear from the long Ru···Ru distance of 3.359 (4) Å. Also the ¹H and ¹³C NMR and IR data of the APP complexes 2a,b are fully compa-rable with those of the earlier reported AIB complexes,[2] which justifies the above-mentioned conclusion that both types of products have similar structures. It therefore seems plausible to assume that the mode of formation of 2a,b is analogous to that of the Ru₂(CO)₆[AIB(R,R′,R″)] complexes. For the latter products it has been proposed that they are formed via a direct electrophilic attack of the alkyne on the C atom of the η²-C=N bonded imine moiety. For the complexes Ru₂(CO)₆[AIB(R,R′,R″)] it is known that they easily and reversibly lose one CO ligand to give the complexes Ru₂(CO)₅[AIB(R,R′,R″)] in which the Ru-Ru bond is restored and one CO group now occupies a bridging position.[2] Such a process has not been observed

(14) Overbeek, A. R.; Schenk, H. *Computing in Crystallography*; Schenk, H., Olthof-Hazekamp, R., van Koningsveld, H., Bassi, G. C., Eds.; University Press: Delft, 1978.

(15) Walker, N.; Stuart, D. *Acta Crystallogr., Sect. A* 1983, *A39*, 158.

(16) Stewart, J. M. The XRAY76 system; Technical Report TR446; Computer Science Center, University of Maryland, College Park, MD, 1976.

(17) Cromer, D. T.; Mann, J. B. *Acta Crystallogr., Sect. A* 1968, *A24*, 321.

(18) *International Tables for X-Ray Crystallography*; Kynoch Press: Birmingham, 1974; Vol. IV.

(19) AIB(R,R′,R″) is the abbreviation for the organic ligand resulting from the C—C bond formation between an R-DAB ligand and an alkyne R′C≡CR″. The backbone of the ligand is RN=C(H)C(H)(NR)C(R′)=CR″, which is 3-amino-4-imino-1-butene.

Scheme I. Reactions of Ru₂(CO)₆(R-Pyca) with Alkynes

1 a R=i-Pr
b R=t-Bu

R'C₂R"
(DMADC, MP: 20 °C
PTA, ethyne: 98 °C)

R'C₂R", 69 °C

2 a R=i-Pr, R'=R"=C(O)OMe
b R=i-Pr, R'=C(O)OMe, R"=H

40 °C

5

-CO

3 a R=i-Pr, R'=R"=C(O)OMe

6

4 a R=i-Pr, R'=R"=C(O)OMe
b R=t-Bu, R'=p-Tol, R"=H
c R=i-Pr, R'=R"=H

7 R=i-Pr, R'=H, R"=C(O)OMe
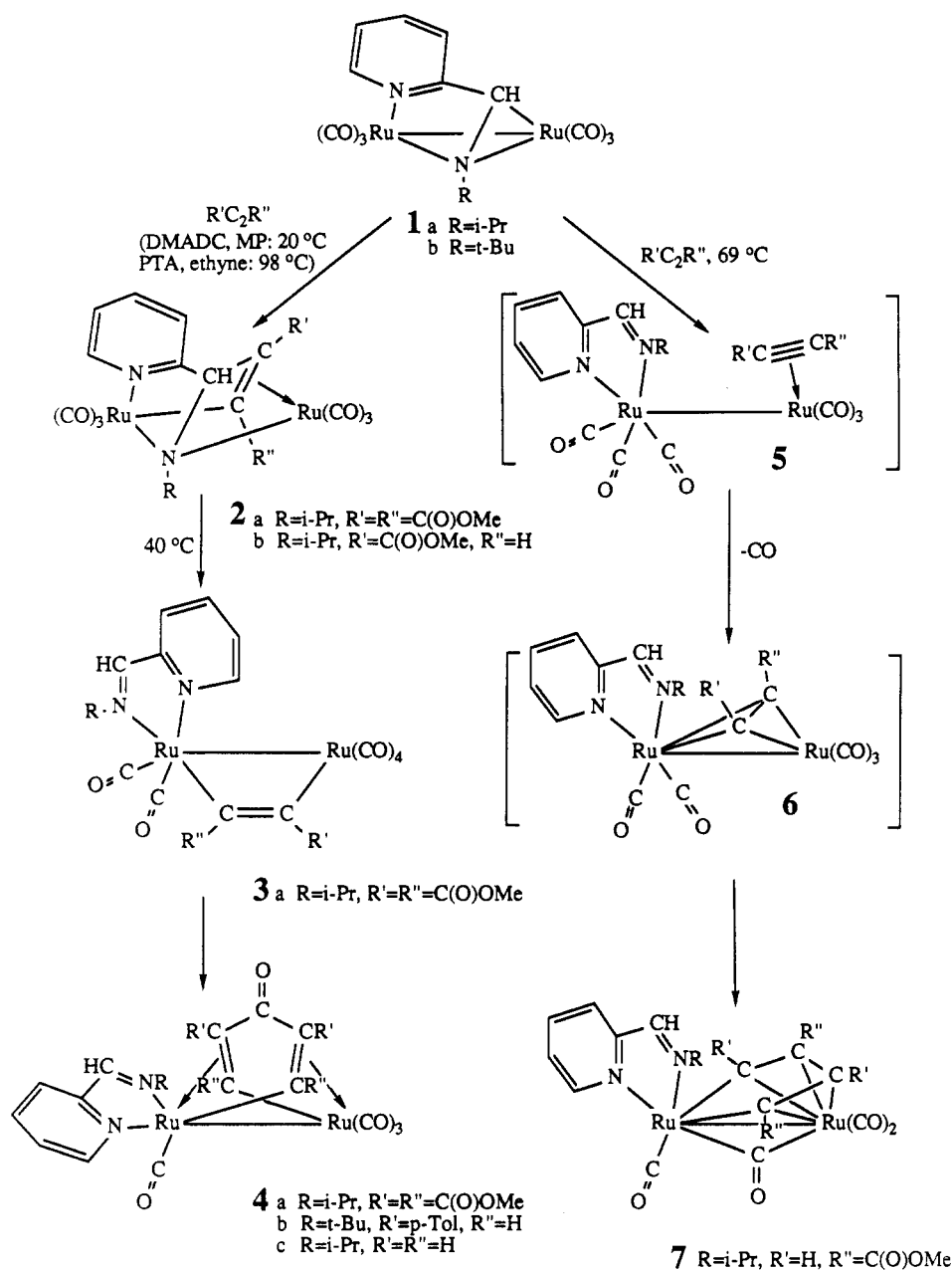
for the presently discussed Pyca derivatives. Instead, when **2b** is heated, extensive decomposition takes place and no defined products could be isolated. Interestingly, **2a** rearranges easily but irreversibly when dissolved in dichloromethane to give Ru₂(CO)₆(*i*-Pr-Pyca)(μ₂-DMADC) (**3**). This complex, which obviously results from the concomitant decoupling of the C–C bond between the alkyne and the Pyca ligand and migration of a CO ligand from one Ru center to the other, is clearly the thermodynamically more stable isomer. Its structural features will be discussed below.

The fact that the APP complex **2a** irreversibly isomerizes to give **3** indicates that the APP complexes are most likely not formed via an initial insertion of the alkyne in the Ru–Ru bond in **1a**, prior to the C–C coupling to give **2**. If such an intermediate with a bridging 6e donating Pyca ligand and a μ₂-bonded alkyne inserted in the Ru–Ru bond would be involved, it would probably rearrange directly to the thermodynamically stable isomer **3**, instead of first making a C–C bond, thus forming **2** and subse-

quently breaking this C–C bond between the imine moiety and the alkyne again to form **3**.

An intriguing question is why the APP complexes **2a,b** do not lose a CO, as is observed for the analogous AIB complexes. Apparently the formed C–C bond in **2** is more easily broken relative to the formed C–C bond in the AIB complexes. A possible explanation for this is that a coordinated APP ligand is destabilized relative to a coordinated AIB ligand, which is the result of the presence of a rigid pyridyl fragment which causes a strain in the Ru₂(CO)₆APP complex.

Complex **3** reacts thermally (40 °C) with a second equivalent of DMADC to give Ru₂(CO)₄(*i*-Pr-Pyca){(C(C-(O)OMe)=(C(O)OMe))₂C(=O)} (**4a**). In this complexes, as was shown by the crystal structure determination (vide infra) both alkynes are C–C coupled with a CO group forming a flyover bridge ligand (see Scheme I). There is no certainty about the reaction route leading from **3** to **4a**, but two possible mechanisms can be put forward. The first is an insertion of a CO molecule in one of the Ru–C σ-
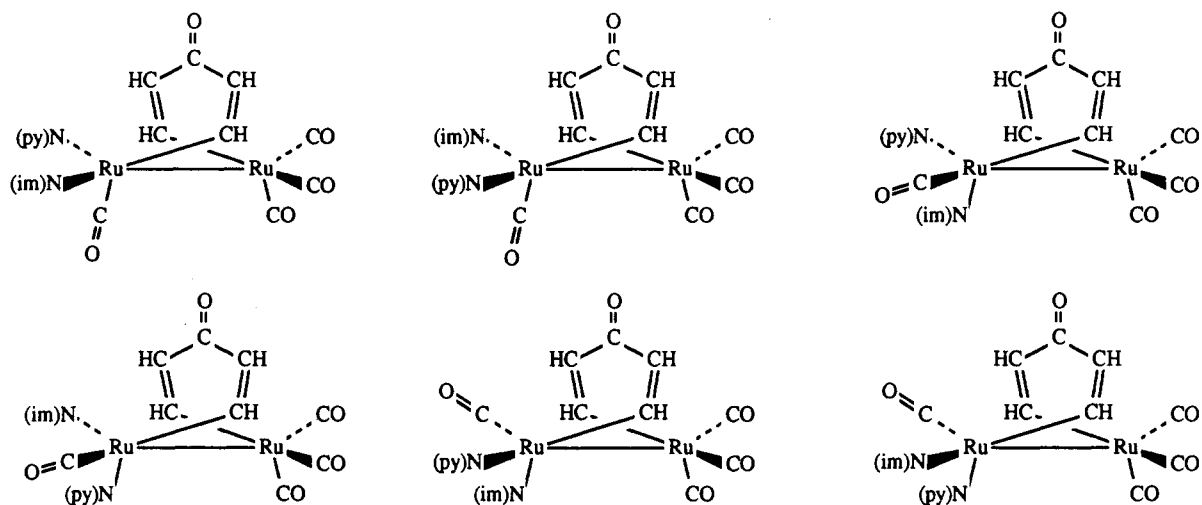
Figure 1. Possible regioisomers of $Ru_2(CO)_4(i\text{-Pr-Pyca})\{HC=CHC(=O)CH=CH\}$ (**4c**).

bonds of the alkyne resulting in a $\mu_2\text{-RC}=CRC(O)$ fragment. Subsequently the second alkyne is coordinated to the complex via the substitution of one of the CO ligands after which the C–C coupling with the $\mu_2\text{-RC}=CRC(O)$ fragment results in the flyover ligand. A second mechanism comprises the initial substitution of a CO ligand by the second DMADC molecule which is C–C coupled with a second CO group. The resulting $\mu_2\text{-RC}=CRC(O)$ fragment finally gives C—C bond formation with the first, μ_2-bridging, alkyne yielding **4a**.

Products isostructural to **4a** were observed in the reactions of 1 with PTA and ethyne, i.e. the complexes Ru_2-$(CO)_4(R\text{-Pyca})\{HC=CR'C(=O)CR'=CH\}$ [**4b**, R = t-Bu, R' = p-Tol; **4c**, R = i-Pr, R' = H]. These complexes also contain a chelating R-Pyca ligand as well as a flyover ligand of the same type as in **4a** formed via the coupling of two alkynes and a CO molecule. In the formation of **4b** and **4c** no intermediate compounds could be isolated or observed, which makes the formulation of a definite mechanism impossible. It seems, however, not unlikely that their formation proceeds via a mechanism similar to that of the formation of **4a**.

The isolated complexes **4b** and **4c**, however, show a number of unusual features. In the case of **4b**, of which the crystal structure will be discussed below, only one isomer is can be isolated, i.e. with the C-p-Tol moieties of the alkynes coupled to the CO groups, whereas normally in the case of asymmetrically substituted alkynes a mixture of isomers is obtained.[20] It seems unlikely to ascribe this regioselectivity to steric factors since the coupling reactions of the alkynes take place on the sterically most hindered C atoms. This suggests that the small electron-withdrawing effect of the p-tolyl substituents is the determining factor in the stereochemical course of the C–C coupling reactions.

Of interest is that the product obtained from the reaction of **1a** with ethyne is a mixture of three isomers (**4c**, **4c'**, and **4c''**). These isomers differ in the orientation of the Pyca ligand with respect to the pentadienonediyl ligand. This could be concluded from the ^1H NMR spectrum of the mixture of **4c,c',c''** of which the resonances due to

the different isomers could be assigned via ^1H–^1H correlated 2D NMR spectroscopy. It was, however, not possible to conclude from the obtained data which three of the six theoretically possible isomers (see Figure 1) were obtained.

Neither was it possible to separate the mixture by further chromatography or crystallization. The formation of this mixture of isomers is most likely due to the small steric demands of the unsubstituted pentadienonediyl fragment when compared to e.g., **4b** where the steric repulsion between the p-tolyl groups and the Pyca ligand causes the isolated isomer to be significantly more stable than the others.

When **1a** and MP are reacted at higher temperature (69 °C), the formation of **2b** competes with a second reaction route. This involves the formation of the ruthenacyclo-pentadienyl complex $Ru_2[C(C(O)OMe)=CHC(C(O)\text{-}OMe)=CH](CO)_4(i\text{-Pr-Pyca})$ (7). The structure of this complex (see Scheme I) is proposed on basis of IR and ^1H and ^{13}C NMR data and consists of a $Ru(CO)_2$ and a Ru-$[C(C(O)OMe)=CHC(C(O)OMe)=CH][CO](i\text{-Pr-Pyca})$ ruthenacyclopentadienyl fragment, which are bridged by one CO ligand. This complex is isostructural with the ferracyclopentadienyl complexes $Fe_2[C_4R'_2(C(O)\text{-}OMe)_2](CO)_4(L)$ [L = R-DAB, R-Pyca; R' = H, C(O)OMe] which are formed in the reactions of $Fe_2(CO)_6(L)$, which are isostructural to 1, with MP or DMADC.[9d] We propose that 7 is formed in a similar fashion as the above-mentioned Fe_2 complexes. The first step in such a mechanism is the substitution of the η^2-C=N coordinated imine moiety in **1a** by an alkyne molecule, thus changing the coordination mode of the Pyca ligand from 6e bridging to 4e chelating. Subsequently this intermediate 5 loses a CO ligand, and the alkyne becomes bonded in the $\mu_2\text{-}\eta^2$-perpendicular coordination mode in intermediate 6. Finally 7 is proposed to be formed via the reaction of 6 with a second alkyne molecule resulting in the C–C coupling to give the metallacycle and the loss of a second CO ligand.

Molecular Structure of $Ru_2(CO)_6(i\text{-Pr-Pyca})(\mu_2\text{-}$DMADC) (3). In the crystals of 3 the asymmetric unit contains two independent molecular of the diruthenium complex as well as one molecule of CH_2Cl_2. The two independent molecules are identical apart from the orientation of the methoxycarbonyl substituents of the DMADC ligand, which is most likely due to crystal packing effects. In the following discussion of the structure therefore only molecule 1 will be discussed.

The molecular structure of 3 consists of a $Ru(CO)_4$ unit and a $Ru(CO)_2(i\text{-Pr-Pyca})$ fragment which are linked by

(20) (a) Aime, S.; Milone, L.; Sappa, E. *J. Chem. Soc., Dalton Trans.* **1976**, 838. (b) Piron, J.; Piret, P.; Meunier-Piret, J.; van Meersche, M. *Bull. Soc. Chim. Belg.* **1969**, *78*, 121. (c) Cotton, F. A.; Hunter, D. .; Troup, J. M. *Inorg. Chem.* **1976**, *15*, 63. (d) Aime, S.; Gobetto, R.; Nicola, G. Osella, D.; Milone, L.; Rosenberg, E. *Organometallics* **1986**, *5*, 1829. (e) Dickson, R. S.; Fallon, G. D.; McLure, F. I.; Nesbit, R. J. *Organometallics* **1987**, *6*, 215.

Table V. Fractional Coordinates and Equivalent Isotropic Thermal Parameters of the Non-Hydrogen Atoms of 3 (Esd's in Parentheses)

atom	x	y	z	U_{eq}, Å^2
Ru(1)	0.23107 (4)	0.35966 (4)	0.34908 (6)	0.0341 (3)
Ru(2)	0.38152 (5)	0.43701 (4)	0.29959 (7)	0.0392 (4)
N(1)	0.1640 (5)	0.4579 (4)	0.4403 (8)	0.042 (4)
N(2)	0.2551 (5)	0.3407 (5)	0.5633 (8)	0.045 (4)
C(1)	0.1317 (6)	0.3059 (5)	0.3211 (10)	0.045 (5)
C(2)	0.2951 (7)	0.2733 (6)	0.2907 (10)	0.049 (5)
C(3)	0.4081 (7)	0.3639 (7)	0.1530 (10)	0.054 (6)
C(4)	0.3372 (7)	0.5009 (7)	0.4383 (10)	0.057 (6)
C(5)	0.4580 (7)	0.3828 (7)	0.4356 (12)	0.061 (7)
C(6)	0.4535 (8)	0.5124 (7)	0.2420 (12)	0.064 (7)
C(7)	0.1180 (6)	0.5187 (6)	0.3767 (10)	0.049 (5)
C(8)	0.0766 (8)	0.5767 (6)	0.4460 (14)	0.066 (7)
C(9)	0.0806 (8)	0.5759 (7)	0.5861 (13)	0.065 (7)
C(10)	0.1253 (9)	0.5147 (8)	0.6533 (13)	0.073 (8)
C(11)	0.1671 (6)	0.4566 (6)	0.5771 (9)	0.046 (5)
C(12)	0.2181 (7)	0.3919 (7)	0.6384 (9)	0.051 (6)
C(13)	0.3045 (7)	0.2714 (8)	0.6231 (11)	0.059 (6)
C(14)	0.3499 (9)	0.2878 (8)	0.7617 (12)	0.075 (8)
C(15)	0.2446 (12)	0.2058 (9)	0.6228 (19)	0.105 (12)
C(16)	0.2145 (6)	0.4143 (5)	0.1639 (9)	0.040 (5)
C(17)	0.2744 (6)	0.4624 (5)	0.1534 (8)	0.042 (5)
C(18)	0.2675 (6)	0.5192 (6)	0.0437 (10)	0.047 (5)
C(19)	0.3402 (10)	0.5896 (9)	−0.1050 (14)	0.084 (9)
C(20)	0.1471 (6)	0.4001 (6)	0.0526 (1)	0.054 (6)
C(21)	−0.0011 (8)	0.3952 (8)	−0.0079 (17)	0.084 (9)
O(1)	0.0755 (6)	0.2681 (5)	0.3022 (10)	0.078 (6)
O(2)	0.3323 (7)	0.2180 (5)	0.2611 (10)	0.084 (6)
O(3)	0.4215 (7)	0.3260 (6)	0.0659 (10)	0.094 (7)
O(4)	0.3171 (6)	0.5420 (6)	0.5231 (10)	0.084 (6)
O(5)	0.5022 (7)	0.3471 (7)	0.5107 (10)	0.099 (7)
O(6)	0.4989 (7)	0.5569 (7)	0.2129 (13)	0.103 (8)
O(7)	0.3412 (5)	0.5346 (6)	0.0010 (9)	0.082 (6)
O(8)	0.2034 (6)	0.5536 (7)	−0.0048 (11)	0.103 (7)
O(9)	0.0688 (5)	0.4106 (5)	0.0936 (8)	0.066 (5)
O(10)	0.1593 (6)	0.3791 (8)	−0.0593 (9)	0.100 (7)
Ru(1)*	0.74688 (5)	0.15301 (4)	0.45299 (7)	0.0362 (3)
Ru(2)*	0.59565 (5)	0.07526 (5)	0.35547 (8)	0.0446 (4)
N(1)*	0.8135 (5)	0.0548 (5)	0.5522 (9)	0.042 (4)
N(2)*	0.7202 (5)	0.1682 (4)	0.6611 (7)	0.044 (4)
C(1)*	0.6888 (8)	0.2411 (6)	0.3800 (9)	0.052 (6)
C(2)*	0.8479 (7)	0.2021 (7)	0.4590 (11)	0.060 (7)
C(3)*	0.5178 (8)	0.0045 (8)	0.2657 (15)	0.072 (8)
C(4)*	0.5240 (7)	0.1250 (8)	0.4828 (14)	0.072 (8)
C(5)*	0.6472 (7)	−0.0012 (7)	0.4867 (12)	0.057 (6)
C(6)*	0.5650 (8)	0.1556 (8)	0.2251 (14)	0.072 (8)
C(7)*	0.8664 (7)	0.0001 (6)	0.4969 (10)	0.051 (6)
C(8)*	0.9113 (8)	−0.0581 (7)	0.5723 (12)	0.063 (7)
C(9)*	0.9015 (9)	−0.0633 (7)	0.7084 (14)	0.075 (8)
C(10)*	0.8503 (9)	−0.0067 (7)	0.7693 (11)	0.063 (7)
C(11)*	0.8071 (8)	0.0526 (6)	0.6872 (11)	0.056 (6)
C(12)*	0.7518 (7)	0.1150 (6)	0.7398 (9)	0.047 (5)
C(13)*	0.6700 (8)	0.2364 (7)	0.7136 (11)	0.065 (7)
C(14)*	0.6298 (9)	0.2195 (8)	0.8472 (11)	0.075 (8)
C(15)*	0.7266 (11)	0.3061 (7)	0.7240 (15)	0.085 (10)
C(16)*	0.7579 (5)	0.1037 (5)	0.2637 (8)	0.038 (4)
C(17)*	0.6985 (6)	0.0547 (5)	0.2310 (8)	0.041 (5)
C(18)*	0.6986 (7)	0.0068 (6)	0.1037 (10)	0.054 (6)
C(19)*	0.6517 (12)	−0.1071 (9)	−0.0103 (16)	0.098 (11)
C(20)*	0.8306 (6)	0.1185 (6)	0.1886 (10)	0.050 (6)
C(21)*	0.8826 (11)	0.2144 (12)	0.0598 (18)	0.112 (13)
O(1)*	0.6564 (7)	0.2974 (5)	0.3370 (9)	0.085 (6)
O(2)*	0.9099(7)	0.2332 (6)	0.4543 (12)	0.095 (7)
O(3)*	0.4714 (7)	−0.0356 (7)	0.2101 (12)	0.109 (8)
O(4)*	0.4837 (7)	0.1551 (6)	0.5596 (12)	0.099 (8)
O(5)*	0.6723 (6)	−0.0471 (6)	0.5584 (11)	0.091 (7)
O(6)*	0.5486 (7)	0.2007 (7)	0.1405 (12)	0.106 (8)
O(7)*	0.6527 (7)	−0.0568 (5)	0.1065 (9)	0.085 (6)
O(8)*	0.7351 (10)	0.0181 (7)	0.0090 (11)	0.123 (10)
O(9)*	0.8154 (5)	0.1863 (6)	0.1247 (9)	0.074 (5)
O(10)*	0.8959 (6)	0.0805 (6)	0.1877 (12)	0.092 (7)
C100	0.0730 (17)	0.1068 (10)	0.8712 (24)	0.141 (17)
C(11)	0.1133 (4)	0.1751 (4)	0.9805 (6)	0.132 (4)
C(12)	0.0037 (4)	0.1519 (5)	0.7385 (6)	0.154 (5)
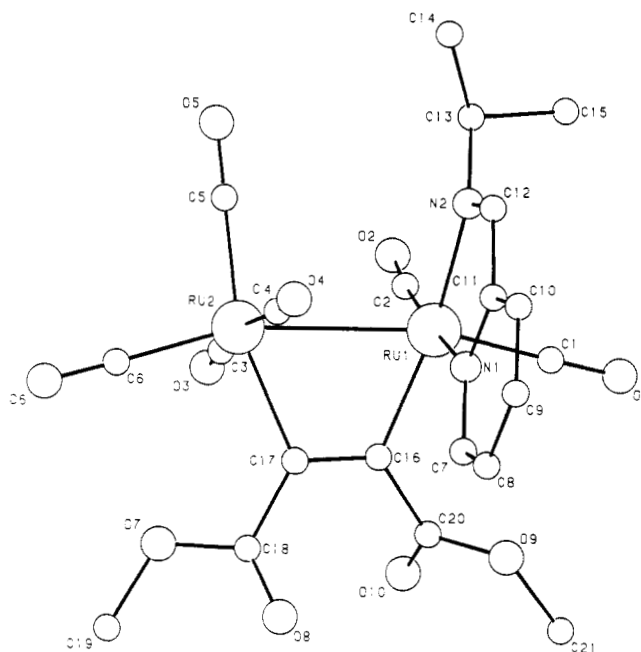
Figure 2. PLUTO drawing molecule 1 of Ru$_2$(CO)$_6$(*i*-Pr-Pyca)(μ_2-DMADC) (3). The H atoms are omitted for clarity.

Table VI. Selected Bond Lengths (Å) of the Non-Hydrogen Atoms of Molecule 1 of 3 (Esd's in Parentheses)

Ru(1)–Ru(2)	2.899 (3)	C(7)–C(8)	1.37 (1)
Ru(1)–N(1)	2.163 (6)	C(8)–C(9)	1.39 (1)
Ru(1)–N(2)	2.158 (6)	C(9)–C(10)	1.38 (1)
Ru(1)–C(16)	2.076 (6)	C(10)–C(11)	1.41 (1)
Ru(2)–C(17)	2.154 (7)	C(16)–C(17)	1.317 (10)
N(1)–C(7)	1.366 (9)	C(16)–C(20)	1.49 (1)
N(1)–C(11)	1.358 (9)	C(17)–C(18)	1.476 (9)
N(2)–C(12)	1.289 (9)	C(11)–C(12)	1.44 (1)
N(2)–C(13)	1.49 (1)		

Table VII. Selected Bond Angles (deg) of the Non-Hydrogen Atoms of Molecule 1 of 3 (Esd's in Parentheses)

Ru(2)–Ru(1)–N(1)	97.5 (2)	C(3)–Ru(2)–C(17)	79.0 (4)
Ru(2)–Ru(1)–N(2)	100.5 (2)	C(4)–Ru(2)–C(5)	89.1 (5)
Ru(2)–Ru(1)–C(1)	161.7 (2)	C(4)–Ru(2)–C(6)	95.7 (5)
Ru(2)–Ru(1)–C(2)	81.9 (3)	C(4)–Ru(2)–C(17)	94.7 (5)
Ru(2)–Ru(1)–C(16)	69.1 (3)	C(5)–Ru(2)–C(6)	100.9 (5)
N(1)–Ru(1)–N(2)	75.7 (3)	C(5)–Ru(2)–C(17)	160.8 (3)
N(1)–Ru(1)–C(1)	91.7 (4)	C(6)–Ru(2)–C(17)	97.4 (5)
N(1)–Ru(1)–C(2)	173.3 (3)	Ru(1)–N(1)–C(7)	127.8 (5)
N(1)–Ru(1)–C(16)	90.2 (4)	Ru(1)–N(1)–C(11)	114.8 (5)
N(2)–Ru(1)–C(1)	97.1 (4)	C(7)–N(1)–C(11)	117.4 (7)
N(2)–Ru(1)–C(2)	97.8 (4)	Ru(1)–N(2)–C(12)	115.0 (5)
N(2)–Ru(1)–C(16)	161.5 (3)	Ru(1)–N(2)–C(13)	124.0 (5)
C(1)–Ru(2)–C(2)	90.8 (5)	C(12)–N(2)–C(13)	120.9 (8)
C(1)–Ru(1)–C(16)	95.2 (4)	N(1)–C(11)–C(10)	122.6 (8)
C(2)–Ru(1)–C(16)	95.8 (4)	N(1)–C(11)–C(12)	114.7 (7)
Ru(1)–Ru(2)–C(3)	92.7 (3)	C(10)–C(11)–C(12)	122.6 (9)
Ru(1)–Ru(2)–C(4)	77.9 (4)	N(2)–C(12)–C(11)	119.7 (8)
Ru(1)–Ru(2)–C(5)	96.4 (4)	Ru(1)–C(16)–C(17)	110.9 (6)
Ru(1)–Ru(2)–C(6)	161.4 (3)	Ru(1)–C(16)–C(20)	126.1 (5)
Ru(1)–Ru(2)–C(17)	66.1 (3)	C(17)–C(16)–C(20)	122.9 (7)
C(3)–Ru(2)–C(4)	170.3 (4)	Ru(2)–C(17)–C(16)	111.1 (6)
C(3)–Ru(2)–C(5)	94.5 (5)	Ru(2)–C(17)–C(18)	127.5 (5)
C(3)–Ru(2)–C(6)	92.5 (5)	C(16)–C(17)–C(18)	121.1 (7)

a formally single Ru–Ru bond [Ru(1)–Ru(2) = 2.899 (3) Å] and bridged by a μ_2-parallel bonded DMADC molecule. The alkyne is slightly twisted with respect to the Ru–Ru axis [C(16)–Ru(1)–Ru(2)–C(17) dihedral angle = 8.2°] which is most likely due to steric influences caused by the

Table VIII. Fractional Coordinates and Equivalent Isotropic Thermal Parameters of the Non-Hydrogen Atoms of 4a (Esd's in Parentheses)

atom	x	y	z	U_{eq}, Å^2
Ru(1)	0.15206 (3)	0.25680 (3)	-0.06452 (4)	0.0300 (2)
Ru(2)	0.13822 (3)	0.09888 (4)	0.04186 (5)	0.0325 (2)
N(1)	0.2074 (3)	0.3517 (4)	-0.1469 (6)	0.041 (3)
N(2)	0.0813 (3)	0.3269 (4)	-0.1762 (5)	0.037 (3)
C(1)	0.1550 (5)	0.0855 (6)	0.2109 (7)	0.054 (5)
C(2)	0.0479 (5)	0.1069 (6)	0.0691 (8)	0.052 (5)
C(3)	0.1389 (4)	-0.0236 (5)	0.0187 (7)	0.045 (4)
C(4)	0.1180 (4)	0.3194 (5)	0.0584 (7)	0.045 (4)
C(5)	0.2776 (4)	0.3643 (5)	-0.1209 (7)	0.046 (4)
C(6)	0.2858 (6)	0.4392 (6)	-0.0356 (11)	0.077 (7)
C(7)	0.3151 (5)	0.3798 (8)	-0.2296 (10)	0.067 (6)
C(8)	0.1778 (4)	0.3957 (5)	-0.2274 (7)	0.044 (4)
C(9)	0.1086 (4)	0.3870 (5)	-0.2463 (7)	0.042 (4)
C(10)	0.0717 (5)	0.4408 (6)	-0.3207 (7)	0.050 (5)
C(11)	0.0058 (5)	0.4328 (7)	-0.3229 (9)	0.061 (6)
C(12)	-0.0218 (5)	0.3751 (7)	-0.2504 (9)	0.058 (5)
C(13)	0.0168 (4)	0.3219 (6)	-0.1789 (8)	0.047 (4)
C(14)	0.2188 (3)	0.1933 (5)	0.0399 (6)	0.036 (3)
C(15)	0.2411 (4)	0.1159 (5)	-0.0079 (6)	0.038 (3)
C(16)	0.2411 (4)	0.1160 (5)	-0.1394 (6)	0.036 (3)
C(17)	0.1796 (4)	0.1548 (4)	-0.1922 (6)	0.034 (3)
C(18)	0.1216 (4)	0.1353 (4)	-0.1302 (6)	0.034 (3)
C(19)	0.2464 (4)	0.2323 (5)	0.1498 (7)	0.043 (4)
C(20)	0.2856 (4)	0.0524 (7)	0.0545 (9)	0.058 (5)
C(21)	0.1732 (4)	0.1845 (5)	-0.3144 (6)	0.042 (4)
C(22)	0.0603 (4)	0.1095 (5)	-0.1948 (6)	0.040 (4)
C(23)	0.3244 (8)	-0.0093 (12)	0.2263 (16)	0.0112 (12)
C(24)	0.3399 (6)	0.3025 (9)	0.2308 (10)	0.082 (8)
C(25)	0.2248 (7)	0.2270 (12)	-0.4803 (10)	0.105 (10)
C(26)	0.0163 (6)	0.0166 (7)	-0.3395 (11)	0.079 (7)
O(1)	0.1603 (5)	0.0738 (6)	0.3048 (6)	0.081 (5)
O(2)	-0.0055 (4)	0.1085 (6)	0.0894 (8)	0.083 (6)
O(3)	0.1435 (4)	-0.0958 (4)	0.0075 (8)	0.071 (5)
O(4)	0.0931 (4)	0.3560 (5)	0.1313 (6)	0.075 (5)
O(5)	0.2858 (3)	0.0909 (4)	-0.1910 (6)	0.057 (4)
O(6)	0.2191 (3)	0.2488 (5)	0.2345 (5)	0.062 (4)
O(7)	0.3057 (4)	-0.0129 (5)	0.0077 (7)	0.076 (5)
O(8)	0.2965 (4)	0.0677 (6)	0.1631 (6)	0.073 (5)
O(9)	0.3077 (3)	0.2572 (5)	0.1330 (6)	0.058 (4)
O(10)	0.1216 (3)	0.2025 (5)	-0.3618 (5)	0.062 (4)
O(11)	0.0064 (3)	0.1335 (5)	-0.1776 (6)	0.060 (4)
O(12)	0.2293 (4)	0.1949 (5)	-0.3634 (6)	0.068 (4)
O(13)	0.0730 (3)	0.0461 (4)	-0.2686 (5)	0.052 (3)
C(32)	-0.0226 (7)	0.3600 (9)	0.4054 (12)	0.088 (4)^a
C(33)	0.0356 (10)	0.3125 (14)	0.3940 (18)	0.132 (6)^a
C(34)	0.0154 (9)	0.2243 (12)	0.3949 (17)	0.114 (5)^a
C(35)	-0.0419 (8)	0.2225 (11)	0.4750 (15)	0.100 (4)^a
C(41)	0.4023 (8)	0.1157 (11)	0.6332 (15)	0.100 (4)^a
O(31)	-0.0723 (7)	0.3124 (9)	0.4417 (12)	0.139 (5)^a
Cl(1)	0.4055 (3)	0.0375 (4)	0.5243 (5)	0.136 (2)^a
Cl(2)	0.4133 (2)	0.2170 (3)	0.5793 (4)	0.102 (1)^a

^{a} Isotropic thermal parameter.

Table IX. Selected Bond Lengths (Å) of the Non-Hydrogen Atoms of 4a (Esd's in Parentheses)

Ru(1)-Ru(2)	2.7630 (6)	N(1)-C(5)	1.475 (8)
Ru(1)-N(1)	2.117 (5)	N(1)-C(8)	1.284 (7)
Ru(1)-N(2)	2.190 (4)	N(2)-C(9)	1.373 (7)
Ru(1)-C(14)	2.039 (5)	N(2)-C(13)	1.330 (8)
Ru(1)-C(17)	2.255 (5)	C(8)-C(9)	1.440 (8)
Ru(1)-C(18)	2.117 (5)	C(14)-C(15)	1.409 (7)
Ru(2)-C(14)	2.216 (5)	C(15)-C(16)	1.519 (7)
Ru(2)-C(15)	2.239 (5)	C(16)-C(17)	1.505 (7)
Ru(2)-C(18)	2.079 (5)	C(16)-O(5)	1.187 (7)
		C(17)-C(18)	1.455 (7)

Table X. Selected Bond Angles (deg) of the Non-Hydrogen Atoms of 4a (Esd's in Parentheses)

Ru(2)-Ru(1)-N(1)	152.5 (1)	Ru(1)-C(14)-Ru(2)	80.9 (3)
Ru(2)-Ru(1)-N(2)	128.5 (1)	Ru(1)-C(14)-C(15)	113.8 (4)
Ru(2)-Ru(1)-C(14)	52.4 (2)	Ru(1)-C(14)-C(19)	121.6 (4)
Ru(2)-Ru(1)-C(17)	72.7 (2)	Ru(2)-C(14)-C(15)	72.5 (5)
Ru(2)-Ru(1)-C(18)	48.2 (1)	Ru(2)-C(14)-C(19)	121.0 (4)
N(1)-Ru(1)-N(2)	75.4 (3)	C(15)-C(14)-C(19)	124.1 (5)
N(1)-Ru(1)-C(14)	103.9 (3)	Ru(2)-C(15)-C(14)	70.6 (4)
N(1)-Ru(1)-C(17)	92.1 (3)	Ru(2)-C(15)-C(16)	107.6 (4)
N(1)-Ru(1)-C(18)	128.0 (2)	Ru(2)-C(15)-C(20)	111.2 (5)
N(2)-Ru(1)-C(14)	179.1 (2)	C(14)-C(15)-C(16)	114.0 (5)
N(2)-Ru(1)-C(17)	98.3 (3)	C(14)-C(15)-C(20)	125.0 (6)
N(2)-Ru(1)-C(18)	93.1 (3)	C(16)-C(15)-C(20)	116.7 (6)
C(14)-Ru(1)-C(17)	82.2 (3)	C(15)-C(16)-C(17)	111.4 (5)
C(14)-Ru(1)-C(18)	87.8 (3)	C(15)-C(16)-O(5)	122.7 (5)
C(17)-Ru(1)-C(18)	38.7 (2)	C(17)-C(16)-O(5)	125.9 (6)
Ru(1)-Ru(2)-C(14)	46.8 (2)	C(16)-C(17)-C(16)	104.4 (4)
Ru(1)-Ru(2)-C(15)	70.2 (2)	Ru(1)-C(17)-C(18)	65.5 (4)
Ru(1)-Ru(2)-C(18)	49.4 (2)	Ru(1)-C(17)-C(21)	113.0 (4)
C(14)-Ru(2)-C(15)	36.9 (2)	C(16)-C(17)-C(18)	114.4 (6)
C(14)-Ru(2)-C(18)	84.2 (3)	C(16)-C(17)-C(21)	122.9 (5)
C(15)-Ru(2)-C(18)	80.6 (3)	C(18)-C(17)-C(21)	119.7 (5)
Ru(1)-N(1)-C(5)	123.0 (4)	Ru(1)-C(18)-Ru(2)	82.4 (3)
Ru(1)-N(1)-C(8)	116.6 (5)	Ru(1)-C(18)-C(17)	75.8 (4)
C(50)-N(1)-C(8)	120.2 (6)	Ru(1)-C(18)-C(22)	130.4 (4)
Ru(1)-N(2)-C(9)	113.9 (4)	Ru(2)-C(18)-C(17)	115.2 (4)
Ru(1)-N(2)-C(13)	128.4 (4)	Ru(2)-C(18)-C(22)	120.1 (4)
C(9)-N(2)-C(13)	117.6 (6)	C(17)-C(18)-C(22)	120.4 (6)

DMADC molecule in μ_2-parallel bridging position. This difference is possibly the result of the presence of the chelating Pyca ligand in **3** where in Os$_2$(CO)$_8$(μ_2-DMADC) there are two terminal CO ligands. The shorter Ru(1)-C(16) distance of 2.076 (6) Å relative to the Ru(2)-C(17) distance of 2.154 (7) Å is very likely related to the trans influence of the N(2) imine donor atom causing an enhanced back-donation from Ru(1) to C(16). A similar asymmetrically bridging DMADC ligand was earlier found in Ir$_2$Cl$_2$(CO)$_2$(μ_2-DMADC)(Ph$_2$PCH$_2$PPh$_2$)$_2$.[21e] Also in this case steric interactions cause the twisting of the alkyne relative to the M–M axis while the M–C bond lengths are influenced by different trans ligands.

Molecular Structures of Ru$_2$(CO)$_4$(i-Pr-Pyca){C$_2$-(C(O)OMe)$_2$C(=O)C$_2$(C(O)OMe)$_2$} (4a) and Ru$_2$-(CO)$_4$(t-Bu-Pyca){HC=C(p-Tol)C(=O)C(p-Tol)=CH} (4b). Only poor quality crystals of **4b** could be obtained, resulting in a limited number of reflections with $I > 2.5\sigma(I)$, which is the reason for the rather large esd's in bond lengths and angles. Therefore it is not possible to draw detailed conclusions regarding bonding interactions in the molecule. Nevertheless the structure determination produced an unambiguous molecular geometry which is worthwhile to compare with those of analogous compounds.

The molecular structures of both **4a** and **4b** consist of a Ru(CO)$_3$ fragment and a Ru(CO(R-Pyca) fragment which are linked by a formally single Ru–Ru bond [**4a**, Ru(1)–Ru(2) = 2.7630 (6) Å; **4b**, Ru(1)–Ru(2) = 2.733 (5) Å] and

asymmetric surrounding of Ru(1). The Ru(1)—C(16) and Ru(2)—C(17) distances of 2.076 (6) and 2.154 (7) Å, respectively, and the C(16)=C(17) double bond distance of 1.317 (10) Å are normal when compared to other dimetallacyclobutene complexes.[21] The geometry of the complex can be described as consisting of two distorted octahedrons, which are slightly twisted (about 20°) along the Ru–Ru axis with respect to each other. This twisting is much more pronounced in **3** than in the isoelectronic complex Os$_2$(CO)$_8$(μ_2-DMADC),[21f] which also contains a

(21) (a) Bennett, M. J.; Graham, W. A. G.; Stewart, R. P., Jr.; Tuggle, R. M. *Inorg. Chem.* **1973**, *12*(12) 2944. (b) Dickson, R. S.; Mok, C.; Pain, G. *J. Organomet. Chem.* **1979**, *166*, 385. (c) Hoffman, D. M.; Hoffmann, R.; Fisel, C. R.; *J. Am. Chem. Soc.* **1982**, *104*, 3858. (d) Mague, J. T.; Klein, C. L.; Majeste, R. J.; Stevens, E. D.; *Organometallics* **1984**, *3*, 1860. (e) Sutherland, B. R.; Cowie, M. *Organometallics* **1984**, *3*, 1869. (f) Burke, M. R.; Takats, J. *J. Organomet. Chem.* **1986**, *302*, C25.
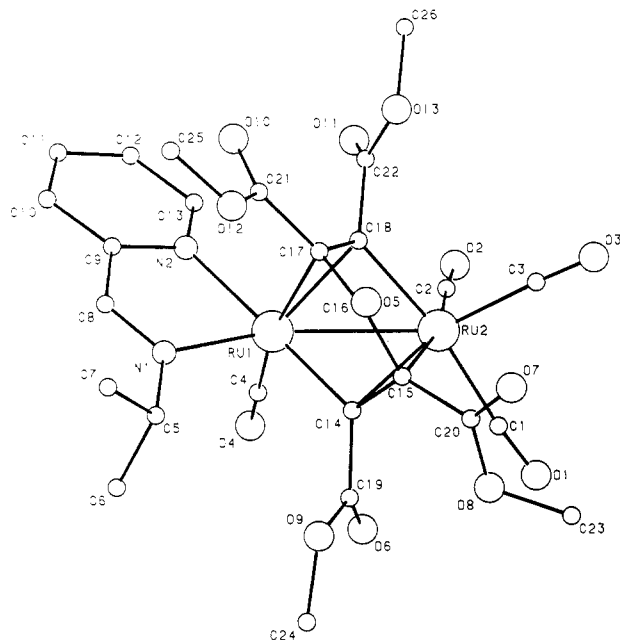
Table XI. Fractional Coordinates and Equivalent Isotropic Thermal Parameters of the Non-Hydrogen Atoms of 4b (Esd's in Parentheses)

atom	x	y	z	U_{eq}, Å^2
Ru(1)	0.5 (0)	0.33586 (7)	0.5 (0)	0.0340 (8)
Ru(2)	0.5350 (2)	0.25583 (7)	0.6770 (2)	0.0411 (9)
C(1)	0.512 (2)	0.439 (1)	0.367 (2)	0.05 (1)
C(2)	0.595 (2)	0.4022 (9)	0.374 (2)	0.04 (1)
C(3)	0.665 (2)	0.308 (1)	0.413 (2)	0.05 (2)
C(4)	0.741 (2)	0.324 (1)	0.369 (3)	0.06 (2)
C(5)	0.743 (3)	0.382 (1)	0.333 (3)	0.07 (2)
C(6)	0.668 (2)	0.421 (1)	0.336 (2)	0.06 (2)
C(7)	0.354 (2)	0.4532 (9)	0.385 (2)	0.04 (1)
C(8)	0.370 (3)	0.478 (1)	0.506 (2)	0.07 (2)
C(9)	0.266 (3)	0.407 (1)	0.335 (2)	0.06 (2)
C(10)	0.336 (3)	0.505 (1)	0.301 (2)	0.08 (2)
C(11)	0.429 (2)	0.3312 (9)	0.602 (2)	0.05 (1)
C(12)	0.490 (2)	0.3481 (9)	0.723 (2)	0.04 (1)
C(13)	0.572 (2)	0.3900 (8)	0.733 (2)	0.04 (1)
C(14)	0.630 (2)	0.3746 (9)	0.672 (2)	0.04 (1)
C(15)	0.638 (2)	0.3120 (9)	0.650 (2)	0.05 (1)
C(16)	0.447 (3)	0.3462 (9)	0.809 (2)	0.06 (2)
C(17)	0.344 (2)	0.339 (1)	0.783 (3)	0.06 (2)
C(18)	0.314 (2)	0.339 (1)	0.877 (2)	0.06 (2)
C(19)	0.385 (2)	0.343 (1)	0.994 (2)	0.06 (2)
C(20)	0.492 (2)	0.352 (1)	1.024 (2)	0.06 (2)
C(21)	0.531 (2)	0.352 (1)	0.941 (2)	0.07 (2)
C(22)	0.346 (3)	0.346 (2)	1.085 (3)	0.10 (3)
C(23)	0.705 (2)	0.4194 (9)	0.661 (2)	0.04 (1)
C(24)	0.670 (3)	0.478 (1)	0.625 (3)	0.08 (2)
C(25)	0.741 (2)	0.516 (1)	0.608 (2)	0.06 (2)
C(26)	0.838 (3)	0.500 (1)	0.630 (4)	0.10 (3)
C(27)	0.865 (4)	0.445 (1)	0.650 (5)	0.13 (4)
C(28)	0.801 (2)	0.403 (2)	0.682 (3)	0.08 (2)
C(29)	0.904 (5)	0.543 (2)	0.602 (7)	0.20 (6)
C(30)	0.422 (2)	0.215 (1)	0.673 (2)	0.06 (2)
C(31)	0.629 (2)	0.2385 (10)	0.839 (2)	0.06 (2)
C(32)	0.570 (2)	0.1947 (10)	0.598 (3)	0.05 (2)
C(33)	0.413 (2)	0.284 (1)	0.389 (3)	0.05 (2)
N(1)	0.452 (2)	0.4182 (8)	0.406 (2)	0.04 (1)
N(2)	0.598 (1)	0.3464 (7)	0.414 (2)	0.030 (10)
O(13)	0.583 (1)	0.4371 (7)	0.794 (2)	0.05 (1)
O(30)	0.348 (2)	0.191 (1)	0.670 (2)	0.09 (2)
O(31)	0.685 (2)	0.231 (1)	0.935 (2)	0.10 (2)
O(32)	0.589 (2)	0.1573 (9)	0.554 (2)	0.10 (2)
O(33)	0.360 (2)	0.2479 (9)	0.320 (2)	0.08 (2)

Figure 3. PLUTO drawing of Ru$_2$(CO)$_4${*i*-Pr-Pyca}{(C(C(O)OMe)=C(C(O)OMe))$_2$C(=O)} (**4a**). The H atoms are omitted for clarity.
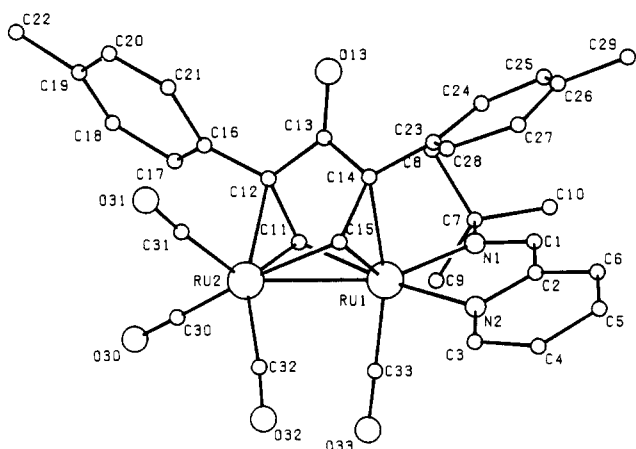
Figure 4. PLUTO drawing of Ru$_2$(CO)$_4${*t*-Bu-Pyca}{HC=C(*p*-Tol)C(=O)C(*p*-Tol)=CH} (**4b**).

Table XII. Selected Bond Lengths (Å) for the Non-Hydrogen Atoms of 4b (Esd's in Parentheses)

Ru(1)–Ru(2)	2.733 (5)	C(1)–C(2)	1.44 (3)
Ru(1)–C(11)	2.00 (2)	C(1)–N(1)	1.27 (3)
Ru(1)–C(14)	2.32 (2)	C(2)–N(2)	1.34 (2)
Ru(1)–C(15)	2.12 (2)	C(3)–N(2)	1.31 (3)
Ru(1)–N(1)	2.13 (1)	C(7)–N(1)	1.55 (3)
Ru(1)–N(2)	2.17 (1)	C(11)–C(12)	1.43 (2)
Ru(2)–C(11)	2.19 (2)	C(12)–C(13)	1.48 (3)
Ru(2)–C(12)	2.32 (2)	C(13)–C(14)	1.43 (3)
Ru(2)–C(15)	2.11 (2)	C(13)–O(13)	1.27 (2)
		C(14)–C(15)	1.44 (2)

bridged by a pentadienonediyl flyover ligand which is bonded to each Ru center via a Ru–C σ-bond and an η^2-C=C coordinated olefinic fragment. The complexes are isostructural and isoelectronic with the known complexes M$_2$(CO)$_6$(RC=CRC(=O)CR=CR) formed in reactions of metal carbonyl clusters with alkynes.[20] Such complexes have been structurally characterized for M = Fe and R = Me or Ph.[20b,c] The presently reported complexes **4a,b** are the first Ru complexes of this type of which the crystal structure has been determined. Complexes **4a** and **4b** differ relative to the structurally characterized Fe complexes with respect to the expected longer M–C bond lengths and the presence of the Pyca ligand instead of two equatorial CO ligands. Furthermore, the pentadienonediyl ligand in **4a,b** is slightly asymmetrically coordinated to the metal carbonyl core. In the case of **4b** this is demonstrated

Table XIII. Selected Bond Angles (deg) of the Non-Hydrogen Atoms of 4b (Esd's in Parentheses)

Ru(2)–Ru(1)–C(11)	52.5 (6)	Ru(1)–N(2)–C(2)	112 (1)
Ru(2)–Ru(1)–C(14)	72.8 (6)	Ru(1)–N(2)–C(3)	127 (1)
Ru(2)–Ru(1)–C(15)	49.5 (6)	C(2)–N(2)–C(3)	120 (2)
Ru(2)–Ru(1)–N(1)	156.5 (4)	Ru(1)–C(11)–Ru(2)	81 (1)
Ru(1)–Ru(1)–N(2)	124.3 (4)	Ru(1)–C(11)–C(12)	115 (2)
C(11)–Ru(1)–C(14)	82 (1)	Ru(2)–C(11)–C(12)	76 (2)
C(11)–Ru(1)–C15)	88 (1)	Ru(2)–C(2)–C(11)	67 (1)
C(11)–Ru(1)–N(1)	105.8 (9)	Ru(2)–C(12)–C(13)	106 (1)
C(11)–Ru(1)–N(2)	170.8 (10)	Ru(2)–C(12)–C(16)	115 (1)
C(14)–Ru(1)–C(15)	37.7 (8)	C(11)–C(12)–C(13)	110 (2)
C(14)–Ru(1)–N(1)	97.1 (8)	C(11)–C(12)–C(16)	121 (2)
C(14)–Ru(1)–N(20)	89.2 (9)	C(13)–C(12)–C(16)	123 (2)
C(15)–Ru(1)–N(1)	131.1 (8)	C(12)–C(13)–C(14)	117 (2)
C(15)–Ru(1)–N(2)	84 (1)	C(12)–C(13)–O(13)	117 (2)
N(1)–Ru(1)–N(2)	75.5 (8)	C(14)–C(13)–O(13)	126 (2)
Ru(1)–Ru(2)–C(11)	46.2 (5)	Ru(1)–C(14)–C(13)	100 (2)
Ru(1)–Ru(2)–C(12)	69.8 (6)	Ru(1)–C(14)–C(15)	64 (1)
Ru(1)–Ru(2)–C(15)	49.9 (6)	Ru(1)–C(14)–C(23)	118 (1)
C(11)–Ru(2)–C(12)	36.9 (8)	C(13)–C(14)–C(15)	117 (2)
C(11)–Ru(2)–C(15)	84 (1)	C(13)–C(14)–C(15)	121 (2)
C(12)–Ru(2)–C(15)	79 (1)	C(15)–C(14)–C(23)	119 (2)
Ru(1)–N(1)–C(1)	115 (1)	Ru(1)–C(15)–Ru(2)	81 (1)
Ru(1)–N(1)–C(7)	125 (1)	Ru(1)–C(15)–C(14)	79 (2)
C(1)–N(1)–C(7)	120 (2)	Ru(2)–C(15)–C(14)	115 (2)

by the shorter Ru(1)–C(11) distance of 2.00 (2) Å when compared to 2.11 (2) Å for Ru(2)–C(15) (see Figure 4). This may be explained by the trans influence of the σ-N donor atom of the Pyca ligand trans to C(11), whereas C(15) is trans to a CO ligand. This is in contrast to **4a**, in which the Ru–C σ-bonds are almost equal [Ru(1)–C(14) = 2.039 (5) Å; Ru(2)–C(18) = 2.079 (5) Å; see Figure 3]. In **4a**, however, the C=C distance of the olefinic fragment π-bonded to the Ru(Pyca) center is longer than the C=C distance of the other olefinic fragment [C(17)–C(18) = 1.455 (7) Å; C(14)–C(15) = 1.409 (7) Å]. This points to a stronger π-back-bonding from the Ru(1) atom to the C-(17)=C(18) fragment, caused by the higher electron density on this Ru atom which is caused by the hard σ-N donor atoms. This is corroborated by the somewhat shorter Ru(1)—C(17)=C(18) distances relative to the Ru(2)—C(15)=C(16) distances. This conclusion, however, conflicts with the results of a theoretical study of Fe$_2$-(CO)$_6$(HC=CHC(=O)CH=CH). This study led to the conclusion that the bonding of the organic ligand to the metal carbonyl core is dominated by the σ-interactions between the metal atoms and the terminal pentadien-onediyl fragment rather than by the π-interaction of the double bonds with the metal atoms.[22]

The orientation of the substituents on the pentadien-onediyl fragment in **4a,b** will be largely determined by the minimalization of steric repulsion with the CO and Pyca ligands. The small dihedral angles C(11)–C(12)–C(16)–C(17) of 11.3° and C(15)–C(14)–C(23)–C(28) of 28.2° in **4b** and C(18)–C(17)–C(21)–O(10) and C(14)–C(15)–C-(20)–O(8) of 8° in **4a** on the other hand suggest that in both complexes the conjugation of the aromatic rings and methoxycarbonyl groups, respectively, with the olefinic bonds may also play an important role.

Conclusions

We have shown that the reaction of Ru$_2$(CO)$_6$(R-Pyca) with alkynes add an interesting new part of chemistry to that observed in the reactions of other dinuclear metal carbonyl α-diimine complexes with alkynes. A part of this Pyca chemistry involves C–C coupling reactions of the

alkyne with the coordinated α-diimine ligand analogous to the Ru$_2$(CO)$_6$(R-DAB)/alkyne chemistry. The formed C–C bond, however, appeared to be significantly less stable than those in the DAB derivatives, which is the reason for the different further reactions of the initially formed Ru$_2$(CO)$_6$APP complexes, when compared to the reactivity of the isostructural Ru$_2$(CO)$_6$AIB complexes. A second important difference with the Ru$_2$(CO)$_6$(R-DAB)/alkyne chemistry is that the η^2-C=N bonded imine moiety is apparently more easily substituted by an alkyne, which is possibly related to the smaller π-accepting capacity of R-Pyca when compared with R-DAB.[23] This reaction path opens the possibility of the formation of products analogous to those found in the reactions of Fe$_2$(CO)$_6$(R-DAB/R-Pyca) with alkynes, in which also the η^2-C=N coordinated imine fragment is easily substituted. An example is the formation of **7** which is the first known ruthenacyclopentadienyl α-diimine complex. The flyover complexes **4a,b** are the first crystallography identified Ru flyover complexes.

Supplementary Material Available: Tables of the anisotropic thermal parameters of the non-hydrogen atoms for **3**, **4a**, and **4b**, tables of the calculated fractional coordinates of the hydrogen atoms for **3** and **4a**, a table of the bond lengths of the non-hydrogen atoms for **3**, full listings of bond angles of the non-hydrogen atoms for **3**, **4a**, and **4b**, and stereoscopic ORTEP representations for **3**, **4a**, and **4b** (14 pages); listings of observed and calculated structure factors for **3**, **4a**, and **4b** (94 pages). Ordering information is given on any current masthead page.

(22) Casarin, M.; Ajo, D.; Granozzi, G.; Bertoncello, R.; Osella, D. *Inorg. Chem.* **1986**, *25*, 511.

(23) Balk, R. W.; Stufkens, D. J.; Oskam, A. *Inorg. Chim. Acta* **1978**, *28*, 133.